A continuous-wave electron–nuclear double resonance (X-band) study of the Cu^{2+} sites of particulate methane mono-oxygenase of *Methylococcus capsulatus* (strain M) in membrane and pure dopamine β-mono-oxygenase of the adrenal medulla

Bettina KATTERLE*[1], Rudolf I. GVOZDEV†, Ntei ABUDU‡, Torbjørn LJONES‡ and K. Kristoffer ANDERSSON*[2]

*Department of Biochemistry, University of Oslo, P.O. Box 1041 Blindern, N-0316 Oslo, Norway, †Institute of Problems of Chemical Physics, Russian Academy of Sciences, Chernogolovka, Noginsk Scientific Center, Moscow region 142432, Russia, and ‡Department of Chemistry, Norwegian University of Science and Technology, N-7491 Trondheim, Norway

All methanotrophic bacteria express a membrane-bound (particulate) methane mono-oxygenase (pMMO). In the present study, we have investigated pMMO in membrane fragments from *Methylococcus capsulatus* (strain M). pMMO contains a typical type-2 Cu^{2+} centre with the following EPR parameters: g_z 2.24, $g_{x,y}$ 2.06, A_z^{Cu} 19.0 mT and $A_{x,y}^{Cu}$ 1.0 mT. Simulation of the Cu^{2+} spectrum yielded a best match by using four equivalent nitrogens ($A^N = 1.5$ mT, 42 MHz). Incubation with ferricyanide neither changed nor increased the amount of EPR-active Cu^{2+}, in contrast with other reports. The EPR visible copper seems not to be part of any cluster, as judged from the microwave power saturation behaviour. Continuous-wave electron–nuclear double resonance (CW ENDOR; 9.4 GHz, 5–20 K) experiments at $g_\perp$ of the Cu(II) spectrum show a weak coupling to protons with an A^H of 2.9 MHz that corresponds to a distance of 3.8 Å (1 Å ≡ 0.1 nm), assuming that it is a purely dipolar coupling. Incubation in ^2H_2O leads to a significant decrease in these ^{1}H-ENDOR intensities, showing that these protons are exchangeable. This result strongly suggests that the EPR visible copper site of pMMO is accessible to solvent, which was confirmed by the chelation of the Cu^{2+} by diethyldithiocarbamic acid. The ^{1}H and ^{14}N hyperfine coupling constants confirm a histidine ligation of the EPR visible copper site in pMMO. The hyperfine structure in the ENDOR or EPR spectra of pMMO is not influenced by the inhibitors azide, cyanide or ammonia, indicating that they do not bind to the EPR visible copper. We compared pMMO with the type-2 Cu^{2+} enzyme, dopamine β-mono-oxygenase (DβM). For DβM, it is assumed that the copper site is solvent-accessible. CW ENDOR shows similar weakly coupled and ^2H_2O-exchangeable protons (2.9 MHz), as observed in pMMO, as well as the strongly coupled nitrogens (40 MHz) from the co-ordinating N of the histidines in DβM. In conclusion, the resting EPR visible Cu in pMMO is not part of a trinuclear cluster, as has been suggested previously.

Key words: CW ENDOR, dopamine β-mono-oxygenase, methane mono-oxygenases, type-2 copper site.

INTRODUCTION

Membrane-bound particulate methane mono-oxygenase (pMMO) and dopamine β-mono-oxygenase (DβM; EC 1.14.17.1) belong to a class of enzymes catalysing a reductive activation of dioxygen, resulting in the insertion of one oxygen atom into a C–H bond and the formation of water. Both enzymes require copper as a cofactor [1–3].

Methanotrophic bacteria have the unique ability to use methane as their sole carbon and energy source. They catalyse oxidation of methane to methanol by using molecular oxygen and reducing equivalents originating from NADH:

$$CH_4 + O_2 + 2H^+ + 2e \rightarrow CH_3OH + H_2O$$

Methanotrophic bacteria are able to express two genetically different forms of MMOs. The membrane-bound form, pMMO, is generally expressed when the copper-to-biomass ratio is high. If the copper-to-biomass ratio is low, the expression can be switched to a soluble form, sMMO, in some methanotrophic species [3]. sMMO is a well-characterized enzyme, which utilizes a di-iron centre for methane oxidation. Several intermediates in the reaction cycle have been trapped and characterized [2]. In pMMO, the number of copper ions involved in catalysis and the structure of the copper centre(s) are still a subject for debate [4–7].

Metal-ion analysis by atomic absorption yields a large number of copper, and possibly iron, ions per pMMO from various methanotrophic species [5–11]. pMMO in cells, in membrane fragments and as purified protein exhibits a typical type 2 non-blue copper EPR spectrum with characteristic g-values and copper hyperfine constants, A^{Cu}s [5–8]. The EPR signal of a type-2 Cu^{2+} (d^9) centre is of the axial type, i.e. $g_z = g_\parallel \equiv 2.2$; $g_x = g_y = g_\perp \equiv 2.0$, since the unpaired electron is located in the $d_{x^2-y^2}$ orbital and the $I = 3/2$ nuclear spins of ^{63}Cu and ^{65}Cu couple anisotropically with $13 < A_\parallel^{Cu} < 19$ mT, and a much smaller unresolved $A_\perp^{Cu}$ of approx. 0.5–2.5 mT.

An X- and S-band EPR study on pMMO in *Methylococcus album* BG8 cells labelled by ^{15}N and substituted with $^{63}Cu^{2+}$ revealed that there are two type-2 copper sites. One is ligated by four histidine residues, and the second by nitrogen donors possibly from the peptide backbone and histidine residues [7,8].

Abbreviations used: (CW) ENDOR, (continuous-wave) electron–nuclear double resonance; DβM, dopamine β-mono-oxygenase; DDTC, diethyldithiocarbamic acid; PAMcc, catalytic core of the peptidylglycine α-amidating enzyme; pMMO, membrane-bound particulate methane mono-oxygenase; rf, radiofrequency; sMMO, soluble MMO; SOD, superoxide dismutase.

[1] Present address: Max Planck Institute of Radiation Chemistry, Stiftstrasse 34–36, D-45470 Mülheim a. d. Rühr, Germany.

[2] To whom correspondence should be addressed (e-mail k.k.andersson@biokjemi.uio.no).

An electron spin echo envelope modulation ('EESEM') study also found histidine ligation to the EPR visible Cu^{2+} centre in *M. capsulatus* (Bath) [9]. Chan and colleagues [9] interpreted their EPR, EXAFS and saturation magnetization data, together with the finding of 15 copper ions per pMMO by atomic absorption spectroscopy, as indicating the presence of trinuclear electron transfer clusters (E-clusters) and trinuclear catalytic clusters (C-clusters) [10,11].

Whereas contradictory hypotheses have been published concerning the pMMO Cu^{2+} site, a vast amount of enzymological and spectroscopic data is available for dopamine β-mono-oxygenase (DβM). DβM from adrenergic nervous tissue and the adrenal medulla is a well-studied enzyme also containing type 2 copper, which catalyses the hydroxylation of dopamine to noradrenaline. The naturally occurring electron donor is ascorbic acid [1,12]:

$$RCH_2CH_2NH_2 + O_2 + 2e^- + 2H^+ \rightarrow RCHOHCH_2NH_2 + H_2O$$

DβM has 32% sequence similarity to the mono-oxygenase catalytic core of peptidylglycine α-amidating enzyme (PAMcc) [13]. PAMcc catalyses the hydroxylation of glycine to give an α-hydroxylated intermediate, and this enzyme is also similar to DβM in the sense that it depends upon active-site copper and the reductant ascorbate. The overall chemical similarity and the sequence homology between these enzymes led to a series of investigations where the copper-binding sites and catalytic mechanisms of PAMcc and DβM were compared [1]. Additionally, PAMcc has been crystallized, and its three-dimensional structure has been solved [14]. Soaking PAMcc crystals with 500 μM Cu^{2+} led to the crystal structure showing occupation in both copper binding sites. The presumed oxygen-activating copper centre in the active site (Cu_B) is ligated by two histidines, one methionine and one water in a distorted tetrahedral fashion. The second copper centre (Cu_A) is located 11 Å (1 Å $\equiv$ 0.1 nm) away from the copper in the active site and is co-ordinated by three histidines in a tetragonal geometry. Both coppers are situated within an 11 Å-wide cleft filled with solvent molecules [14]. Site-directed mutagenesis of the methionine to cysteine, histidine, etc. destroys the catalytic activity of PAMcc [15,16]. The methionine residue in the PAMcc crystal structure is 2.7 Å away from Cu_B. From EXAFS analyses, it is known that the methionine comes closer upon reduction to Cu(I), decreasing the bond length to only 2.2 Å [17]. Interestingly, there was no evidence that the substrate co-ordinated with Cu(I)B in the EXAFS studies. This is in accordance with the crystal structure of the catalytic core of PAMcc [14].

The number of coppers (one or two copper ions per monomer) involved in DβM catalysis is still being discussed. Biochemical data have been presented [12] suggesting that only one copper per subunit (pH = 7, $k_{ass} = 10^{11}$; Cu_B) for DβM is sufficient for the full activity of the enzyme, with the second copper ion (pH = 7, $k_{ass} = 10^7$; Cu_A) being bound adventitiously. Other work has suggested that Cu_A binds ascorbate and transfers electrons into the active site, and that Cu_B catalyses the oxygen insertion into the substrate [1].

On the basis of EPR studies, DβM exhibits a typical type-2 cupric site, regardless of whether the enzyme is reconstituted with one or two Cu^{2+} per monomer. The temperature-dependence of the microwave power saturation behaviour suggests that the two coppers are not magnetically interacting, indicating that they are at least 7 Å apart [18], in agreement with the crystal structure of PAMcc, in which a distance of 11 Å was found between the two coppers. EPR, ESEEM, EXAFS and Fourier-transform infrared ('FTIR') studies on DβM have shown that the two mononuclear copper sites can be distinguished by using copper-binding ligands, such as azide or cyanide [19,20]. From these investigations, it was concluded that each Cu^{2+} centre is ligated by two or three histidine ligands and one or two O/N ligands [17,21].

We were interested in a comparison of the cupric sites in DβM and pMMO. Both enzymes show a similar inhibition pattern when treated with chelators such as EDTA, diethyldithiocarbamic acid (DDTC) or small ligands, such as azide. The explanation for the inhibition might be different for the two enzymes. In this study, we present for the first time continuous-wave electron–nuclear double resonance (CW ENDOR) data for pMMO and DβM. ^2H_2O-exchangeable protons can be detected, indicating that the EPR visible Cu^{2+} site of pMMO is accessible to solvent. By comparison with small model complexes, such as $Cu(imidazole)_4$ and $Cu(NH_3)_4$, we found ^{14}N hyperfine couplings of ligating (A_l^N) and remote (A_r^N) nitrogens of the histidine rings in pMMO and DβM. We suggest that the EPR-active Cu^{2+} site in pMMO is not part of a cluster. Furthermore, it might possibly have an electron-transfer role, on the basis of the lack of binding of small typical copper ligands.

EXPERIMENTAL

Cell growth and preparation of pMMO

M. capsulatus (strain M) was grown continuously in a 40 l fermenter at 42 °C, pH 5.6. The growth medium (one litre) contained 0.35 ml of 70% (v/v) H_3PO_4, 0.125 g of KCl, 0.105 g of $MgSO_4 \cdot 7H_2O$, 10 mg of $CuSO_4 \cdot 5H_2O$, 10.75 mg of $FeSO_4 \cdot 7H_2O$, 9.5 mg of $MnSO_4 \cdot 4H_2O$, 6.25 mg of H_3BO_3, 1.5 mg of $ZnSO_4 \cdot 7H_2O$, 0.25 mg of Na_2MoO_4 and 0.25 mg of $CoSO_4$. The pH 5.6 was adjusted with a 10% (v/v) ammonia solution. The flow rate was 100 l/h for methane and 300 l/h for air. The flow rate for the medium was 0.1–0.25 l/h.

After harvesting, the cells (yield = 5 g of dry cells/litre) were centrifuged at 12000 ***g*** at 4 °C, and washed twice with 25 mM sodium phosphate buffer, pH 7.0. The washed cells were immediately disintegrated with a semi-automatic disintegrator (DKM-6; produced in the Institute of Chemical Physics, Russian Academy of Sciences). The crude extract was centrifuged at 3500 ***g*** for 30 min to remove cell debris and unbroken cells, and the supernatant was centrifuged at 90000 ***g*** for 1 h. The pellet was suspended in 25 mM sodium phosphate buffer, pH 7.0, and frozen in liquid nitrogen. The total protein concentration was 30–60 mg/ml, as determined by the standard Bio-Rad, Bradford or Pierce bicinchoninic acid protein assays, or the classical Biuret assays [22].

Activity assay

Activity assays were performed with methane as the substrate. A 3 ml gas-tight vial was filled with an air-saturated protein solution without leaving any gas space. Then, 200 μl of methane-saturated solution was injected into the protein solution. The reaction was started with addition of NADH. After 30 s reaction time, 50 μl of the protein solution was taken out and injected into an empty 3 ml gas-tight vial. The remaining methane immediately diffuses into the head space, from which aliquots were injected into a gas chromatograph. The control sample at $t = 0$ min serves as the reference for the quantification of methane. The activity was in the range 150–300 nmol of CH_4/mg of protein per min at 43 °C [22]. The activity assay of pMMO from *M. capsulatus* (strain M) performed with propene as the substrate at 45 °C yielded an activity that was comparable with pMMO-containing membrane fragments of *M. capsulatus* (Bath) ([23]; personal communication

from P. Basu and H. Dalton, Department of Haematology, University of Cambridge, Cambridge, U.K.).

Quantification of the copper ions

EDTA-washed plastic containers were used to store all Chelex-100-treated solutions, cells, membrane fragments and proteins. Total Cu content of the membranes was determined with atomic absorption spectrometry using a Zeiss AAS-1 spectrometer (Carl Zeiss Jena GmbH, Jena, Germany); the membranes were dissolved in 1 M NaOH and quantified using a $CuSO_4$ standard dissolved in copper-free 1 M NaOH. Subsequently, the membranes were then either dissolved in 0.2 M KOH/1 % (w/v) cholate/10 mM EDTA and incubated at 60 °C for 30 min, or incubated with 10 mM hydrogen peroxide at 25 °C for 30 min and, for the latter two steps, the EPR-active Cu were determined. Alternatively, the membranes were dissolved in 1 M KOH/1 % cholate and incubated at 90 °C for 30 min, before quantification using $CuSO_4$ as the standard dissolved in copper-free 1 M KOH and cholate with 2 mM bathocuproinedisulphonic acid at pH 7 with 10 mM ascorbate [12].

$$\nu_{\pm}(m_I) = \nu(\mathrm{J}) \pm \frac{A(\mathrm{J})}{2} + \frac{3P(\mathrm{J})}{2}(2m_I - 1)$$

$$\nu_{\pm}(m_I) = \nu(\mathrm{J}) \pm \frac{A(\mathrm{J})}{2} + \nu(\mathrm{J}) + \frac{3P(\mathrm{J})}{2}(2m_I - 1)$$

Purification of DβM and ^2H_2O exchange

Apo-DβM from adrenal medulla was purified as described previously [12]. The protein was dissolved in 50 mM Mes, pH 6.5/50 mM KCl. Protein concentration was determined from the absorbance at 280 nm; a solution of 1 mg/ml DβM has an absorbance of 1.24 (light path 10 mm). DβM was concentrated with a Centricon 100 from Amicon to a concentration of approx. 20–30 mg/ml.

For ^2H_2O-exchange experiments, a small column was packed with 1 ml of Sephadex G-25 and equilibrated with 10 ml of 50 mM Mes, p^{2}H 6.5/100 mM KCl in ^2H_2O. The equilibrated columns were then centrifuged in a bench-top centrifuge (GS-15R; Beckman, Fullerton, CA, U.S.A.) for 3 min (3000 rev./min, 4 °C). Of the protein samples, 100 μl was loaded on the column and centrifuged for 3 min at 3000 rev./min. After exchange, the protein was reconstituted with 4, 6 or 8 copper ions per tetramer dissolved in ^2H_2O. The ^2H_2O-exchanged sample was incubated further for 1–2 h at 4 °C.

For the membrane fragments containing pMMO, exchange to ^2H_2O was achieved by repeatedly washing the membrane fragments with 50 mM Pipes, p^{2}H 7.0, in ^2H_2O, and centrifuging at 100 000 ***g*** and 4 °C for 1 h.

X-band EPR spectroscopy, CW ENDOR spectroscopy and data collection

Low-temperature EPR experiments (5–10 K) were performed with a Bruker ESP300E spectrometer operating at X-band frequency (9.6 GHz) equipped with an ER900 liquid-helium cryostat (Oxford Instruments, Oxford, U.K.). The EPR spectra were simulated with *WinSimfonia* (Bruker, Karlsruhe, Germany). For ENDOR (ESP 360D-S from Bruker; 9.4 GHz) measurements, the microwave power was adjusted to 5–10 mW. The ENDOR radiofrequency (in MHz) (rf) components consist of a Wavetek frequency synthesizer and a 300 W ENE broad band rf amplifier. The microwave/rf probe consists of a Bruker cylindrical TM0011 cavity and an rf helix. The rf helix has 14 turns of copper ribbon wrapped around a quartz cryostat finger. ENDOR spectra were observed by fixing the magnetic field at an EPR resonance and by applying partially saturating microwave power while sweeping the NMR transition with an rf source. The rf source was frequency-modulated; therefore the spectral output appears as the derivative of the absorption with respect to frequency. The ENDOR spectra were examined over a frequency range of 1–50 MHz. Wherever possible, several different ENDOR field positions spanning the EPR powder spectrum were used, as shown in Figure 1 for the two enzymes.

For a single orientation of a paramagnetic centre, the ENDOR spectrum of a nucleus (J) with spin I consists, in principle, of $2I$ transitions:

$$\begin{aligned} &\nu(\mathrm{J}) > A(\mathrm{J})/2 \\ &\qquad -I+1 \leqslant m_I \leqslant I \\ &\nu(\mathrm{J}) > A(\mathrm{J})/2 \end{aligned} \tag{1}$$

Here, A(J) and P(J) are the angle-dependent hyperfine and quadrupole-coupling constants respectively, which are molecular parameters and independent of the microwave frequency, and ν(J) is the nuclear Larmor frequency $h\nu(\mathrm{J}) = g_J\beta_J\mathbf{B}$. For a set of equivalent ^{14}N nuclei [$I(^{14}\mathrm{N}) = 1$; $A(^{14}\mathrm{N})/2 > \nu(^{14}\mathrm{N}) > 3P(^{14}\mathrm{N})/2$], eqn (1) describes a quartet centred at $A(^{14}\mathrm{N})/2$ consisting of a doublet split by $2\nu(^{14}\mathrm{N})$ (Larmor split), which is split further by the quadrupole term. For Cu-bound histidine, the quadrupole interaction commonly is not resolved. Here, it is important to note that the maximum possible quadrupole splitting of metal-co-ordinated histidine nitrogen is $3P_{max} \approx 3.3$–3.5 MHz [24,25]. As the ^{14}N resonances are centred on the molecular parameter, $A/2$, the centre of these patterns, does not change with the spectrometer frequency.

A set of magnetically equivalent protons [$I(^1\mathrm{H}) = 1/2$], however, gives a hyperfine-split doublet of ENDOR transitions ($\nu_{\pm}$) that are centred at the proton Larmor frequency $\nu(^1\mathrm{H})$ and split by $A(^1\mathrm{H})$:

$$\nu_{\pm} = \nu(\mathrm{H}) \pm \frac{A(\mathrm{H})}{2} \tag{2}$$

where $\nu(^1\mathrm{H}) = g_H\beta_N\nu(\mathrm{M})/g_{obs}\beta_e$ varies with the microwave frequency, ν(M).

RESULTS

Copper content of highly active pMMO membrane fragments

The pMMO activity is dependent on EPR-active and EPR-silent copper [4–10,22], and therefore we investigated our pMMO-rich membranes for Cu content. Typically, we found a total protein concentration in the membrane fragments of 30 mg/ml, and the resting EPR visible [Cu^{2+}] was approx. 50–100 μM, i.e. approx. 1.5–3.3 nmol of EPR visible [Cu^{2+}]/mg of protein. The amount of EPR-active Cu^{2+} after denaturation of the protein could be increased by approx. 53 % after incubation with 10 mM hydrogen peroxide, or by treatment with 0.2 M KOH/1 % cholate/10 mM

EDTA. This copper concentration was in the range determined by bathocuproinedisulphonate and ascorbate without EDTA. Atomic absorption spectroscopy measurements of different membrane fragments yielded a total copper content of 7.5–11 nmol of copper/mg of protein, using the insensitive Biuret method as the protein assay. Comparison of the copper concentrations measured by EPR and atomic absorption reveals a significant difference. Considering the error in the concentration determinations of membrane samples, and the uncertainty of the concentration of pMMO, the data indicate the presence of some EPR-silent copper in our membrane preparation. On the basis of propene oxide formation, the *M. capsulatus* (strain M) membranes had an activity similar to those of the *M. capsulatus* (Bath) in the range of 50–110 nmol/min per mg of protein [22], whereas the specific activity measured with methane consumption was approx. 150–300 nmol/min per mg of protein. Thus the activity of *M. capsulatus* (strain M) was comparable with the preparation of *M. capsulatus* (Bath) membranes, although it had the lower (2–30-fold lower) Cu : protein ratio, measured either as total Cu in the membrane or as EPR-active Cu^{2+} in pMMO membranes from the studies reported to date [6,8].

EPR studies of pMMO

Figure 1 shows representative X-band EPR spectra from the copper site of pMMO from *M. capsulatus* (strain M) (Figures 1A and 1C), a strain expressing solely pMMO. The membrane fragments contained active pMMO ($M_r = 47000$, 27000 and 25000) as one of the major proteins, as judged from SDS/PAGE (results not shown), in agreement with results from other laboratories [4–10,22]. These membranes contain an additional membrane-associated methanol dehydrogenase, which has a pyrroloquinoline quinone radical (seen as a narrow singlet at $g = 2.00$). A contamination by manganese(II) of $< 10\,\%$ can be seen most clearly at B = 355 mT (marked with an asterisk in Figure 1A, and at 341 mT in Figure 1C).

Simulation of the Cu^{2+} EPR spectrum of pMMO

Figure 1(A) shows the pMMO Cu^{2+} EPR spectrum at 100 mW and 10 K, where the quinone radical is saturated. The overall shape of the Cu^{2+} spectrum is the same under saturating and non-saturating conditions. This Cu^{2+} spectrum exhibits a typical type-2 Cu^{2+} signal, and matches well the simulation using the g and A^{Cu} values listed in Table 1 (the line-width is 5, 5, 6.5 mT for the 100 mW spectrum in Figure 1A). The hyperfine $A_{\perp}^{Cu}$ splittings (0.5–2.5 mT; Table 1) are not usually resolved because of the broad line-width. The EPR spectrum measured at 100 mW shows a small contamination by another type-2 copper, which is slightly visible in the parallel region at 310, 325 mT. The contribution of this copper species is not visible under non-saturating conditions, as shown with the EPR spectrum measured at 50 μW. Measured under non-saturating conditions (2.5 μW), the superhyperfine couplings (A^N) of Cu-co-ordinating nitrogen ligands are resolved with isotropic coupling constants of approx. 1.5 mT (≈ 42 MHz). Simulations of this spectrum give a best match to the data determined experimentally by using three or four equivalent nitrogens. A low amount of a similar type-2 copper would not make a contribution in the perpendicular region at 50 μW, and thus would not influence the intensities of superhyperfine couplings in Figure 1(C). The difference in a simulation including three or four nitrogens is so small that our measured spectrum matches either simulation. The spectral features of the copper site(s) is/are nearly identical with those already described for copper site(s) of pMMO found in other bacterial sources (Table 1).

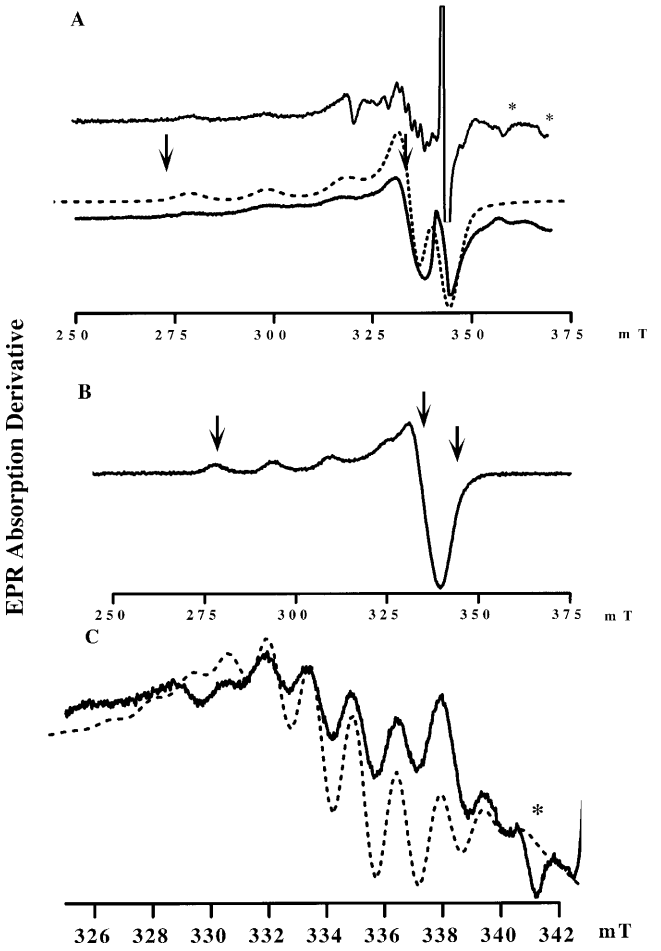

Figure 1 X-band EPR spectra of the cupric site of pMMO in membrane fragments and of DβM at 10 K

(**A**) The pMMO Cu^{2+} spectrum is recorded (continuous lines) at 0.05 (upper trace) and 100 mW (lower trace). The interference of an organic radical from the methanol dehydrogenase is prevented at 100 mW, which is completely saturated under this condition. (**B**) The type-2 Cu^{2+} EPR spectrum of DβM recorded at 100 μW. DβM was reconstituted 8 Cu^{2+} per tetramer. The trace in (**C**) was recorded at 2.5 μW, showing the $g_{\perp}$ region of the Cu^{2+} site of pMMO with its hyperfine structure. Contaminating manganese(II) is marked with asterisks (*). The dotted lines are simulated EPR spectra. In (**A**), the EPR parameters given in Table 1 were used; in addition, the line-width was 5, 5, 6.5 mT. In (**C**), four equal nitrogens were used for the pMMO simulation; all the EPR parameters are shown in Table 1. The magnetic field positions used in ENDOR spectroscopy are indicated by arrows. Recording conditions are: temperature, 10 K; modulation frequency, 100 kHz; modulation amplitude, 0.5 mT; receiver gain, 1×10^5.

Oxidation of pMMO with $K_3Fe(CN)_6$ and addition of inhibitors

In earlier studies by Chan and colleagues [10], pMMO was incubated with $K_3Fe(CN)_6$ and an increase in the EPR-active Cu^{2+} was reported. Incubation of the membrane fragments with 0.2 mM $K_3Fe(CN)_6$ for 30 min did not change significantly the amount of measurable Cu^{2+} present (results not shown). This indicated that, under these conditions, almost no readily oxidizable Cu^{1+} was present in the isolated membrane fragments. In pMMO, the EPR-detectable copper was proposed to be part of the oxygen-binding/activating site [4]. However, the addition of known inhibitors that are able to bind to freely accessible metal sites used to probe oxygen-binding sites on Cu^{2+}, such as azide, F and CN , at a concentration of 5 mM did not change the spectral features ($A_{\parallel}^{Cu}$ or A^N) of the copper site(s) in *M. capsulatus* (strain M; results not shown). Furthermore, no change

Table 1 EPR parameters obtained by simulation of the EPR spectra of pMMO and DβM compared with small model complexes

The hyperfine couplings are given in mT. The power saturation behaviour $P_{1/2}$ was evaluated at 10 K. $Cu(Im)_4$, Cu(imidazole)$_4$; $Cu(gly)_2$, Cu(glycine)$_2$.

Protein–model complex	$g_{\parallel}$	$g_{\perp}$	$A_{\perp}^{Cu}$	$A_{\parallel}^{Cu}$	$A_{\perp}^{N}$	$A_{\parallel}^{N}$	$P_{1/2}$ (μW)
DβM* (bovine adrenal medulla)	2.287	2.056	0.5	15.5			150
pMMO† [*M. capsulatus* (strain M)]	2.24	2.06	1.0	19.0	1.5	1.5	100
pMMO‡ (*M. album* BG8)	2.243	2.059, 2.061		18.5	1.8, 2.0	1.8, 2.0	
pMMO§ [*M. capsulatus* (Bath)]	2.25	2.06		18.5	–	–	
$Cu(Im)_4$‖	2.262	2.051	2.2	17.8	1.17	1.48	
$Cu(NH_3)_4$‖	2.241	2.047	2.4	18.7			
$Cu(gly)_2$‖	2.267	2.052	1.5	16.7			
Cu(DDTC)¶	2.094	2.0274	4.5	17.0			

* The line-width was 4.5, 4.5, 5.0 mT and the line-shape was 40% Gaussian, 60% Lorentzian; EPR parameters from [19].
† The line-width is 1.0, 1.0, 6.5 mT and 100% Gaussian line-shape; the present study.
‡ Parameters are given in [7], parameters are given for two slightly different type-2 coppers.
§ Parameters are given in [10].
‖ Parameters from reference [24].
¶ The line-width was 0.9, 0.9, 1.5 mT and 100% Gaussian line-shape [26].

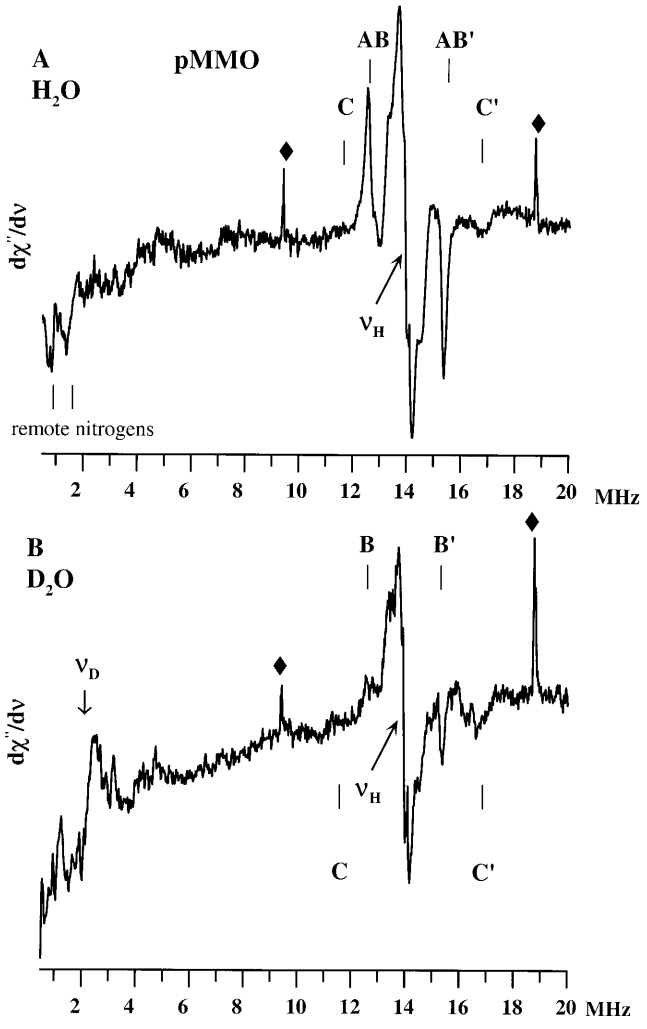

Figure 2 X-band ^{1}H-ENDOR spectra of the cupric site in pMMO at 10 K

The spectra were recorded (**A**) in H_2O and (**B**) in ^2H_2O measured at EPR field position $g_{\perp}$ (denoted by the arrow on the right in Figure 1A). The peaks marked with ◆ are artefacts of the instrument. The EPR visible concentration of Cu^{2+} in the membrane fragments was 150–180 μM.

in the EPR spectrum was observed in the presence of 5 mM ammonia, a known inhibitor of methane oxidation that is able to serve as an alternative substrate (results not shown). This result indicates that they do not bind to the EPR-visible Cu^{2+} site of pMMO.

EPR measurements of DβM

The X-band EPR parameters of the type-2 copper site of DβM are given in Table 1. Its EPR spectrum is shown in Figure 1(C). Comparison with pMMO shows that both Cu^{2+} sites exhibit axial geometry, but the parallel hyperfine coupling constants $A_{\parallel}^{Cu}$, as well as the $g_{\parallel}$, values differ significantly. Furthermore, the superhyperfine couplings of the copper ligands, e.g. histidines, are not resolved in the $g_{\parallel}$ region of the EPR spectrum of DβM containing 4 or 8 Cu^{2+}/tetramer (Figure 1C).

Microwave power saturation behaviour of DβM and pMMO

The microwave power saturation behaviour of the Cu^{2+} EPR signals at 10 K was similar for both enzymes, with a $P_{1/2}$ of 150 ± 20 μW for DβM and 100 ± 5 μW (given as means $\pm$ S.D.) for pMMO. This relaxation behaviour is what is expected for a mononuclear site, as shown for DβM, and strongly indicates that the Cu^{2+} site in pMMO is mononuclear. Neither the line-shape nor the line-width of the EPR spectrum of the DβM monomer are influenced to a great extent by binding of a second copper and, furthermore, the power saturation behaviour is unchanged. For DβM, it is known that azide and CN bind to the coppers, as indicated by spectral changes in the $g_{\perp}$ region of their EPR spectra. In spite of the changes in the direct ligating co-ordination sphere, the power saturation parameter $P_{1/2}$ does not change for DβM [18]; neither does it change for pMMO (results not shown). This mononuclear behaviour and absence of small ligand binding to the copper of pMMO, together with the absence of easily oxidizable Cu^{1+}, indicates that the EPR visible copper in the pMMO complex seems not to be part of a cluster.

ENDOR spectroscopy of DβM, and pMMO ^{1}H-ENDOR spectroscopy

The field positions used for ENDOR experiments are indicated by arrows in Figures 1(A) and 1(B). At $m_I = +3/2$ in the low-

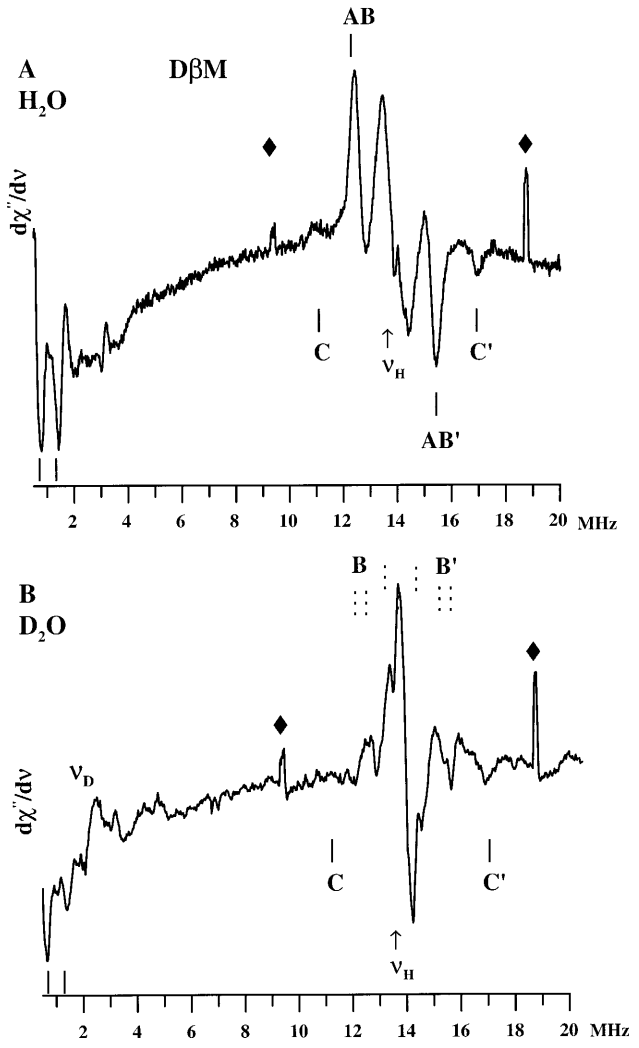

Figure 3 X-band ^{1}H-ENDOR spectra of the cupric sites of DβM reconstituted with 8 Cu^{2+} per tetramer DβM at 10 K

Reconstitution with 4 or 6 Cu^{2+}/tetramer yields exactly the same ENDOR spectrum. (**A**) DβM was reconstituted in H_2O buffer, and in (**B**) the enzyme was reconstituted in ^2H_2O buffer. The peaks marked with ◆ are artefacts of the instrument. EPR field position $g_\perp$ is denoted by the centre arrow in Figure 1(B).

field EPR position of the $g_\parallel$ region of the Cu^{2+} spectrum (arrows located on the left in Figures 1A and 1C), it was not possible to observe any ENDOR response for DβM or pMMO due to low intensity. This is unfortunate, since ENDOR performed at the $g_\parallel$ extreme would give rise to a 'crystal-like' ENDOR spectrum, whereas at $g_\perp$ it is 'powder-like', i.e. many orientations are contributing to the spectrum.

Figures 2 and 3 show the X-band CW ENDOR spectra of the cupric sites of pMMO and DβM (two coppers/monomer respectively), at the maximum of the EPR envelope. They give almost identical resonances in the range 0.5–20.5 MHz. The ^{1}H-ENDOR spectrum of pMMO (Figure 2A) is somewhat better resolved than that of DβM (Figure 3A), e.g. protons with A of 1–2 MHz are detectable as 'shoulders'. The position of the nuclear Zeeman frequency, ν_H, is indicated in each spectrum. Magnetically coupled protons are expected to produce a pair of lines centred at ν_H and displaced by half of the value of the hyperfine coupling. We note that DβM and pMMO display a

Table 2 Hyperfine couplings A found by X-band CW ENDOR spectroscopy given in MHz

A_l^N is the hyperfine coupling constant for the ligating nitrogens and A_r^N for the remote nitrogens in a histidine ring. n.d., not detected.

Protein	$A(H^{a,a'})$	A_l^N	$A(H^{b,b'})$	A_r^N
DβM	2.9	40	6	0.7
pMMO (strain M)	2.9	n.d.	6	0.7

major ^{1}H interaction labelled AB and AB′ that has a coupling constant of 2.9 MHz (Table 2). This indicates a weakly coupled proton in the vicinity of the Cu^{2+} site. All directions of space contribute to the maximum of the EPR envelope, at which our ENDOR spectra were recorded. Therefore we assume that the position of the ENDOR reflects the largest value of the super-hyperfine coupling tensor. Assuming purely dipolar coupling, this is equal to A_{dip}, and one can calculate the maximum distance of the proton using eqn (3):

$$r = \left(\frac{\mu_0 g_e g_N \beta_e \beta_N}{4\pi A_{dip}} \right)^{1/3} \quad (3)$$

Here, $g_e \approx 2$, $g_N = 5.585$, β_e and β_N are the electron and nuclear magnetons respectively, $A_{dip} = A^H = 2.9$ MHz is the dipolar coupling, and μ_0 is the vacuum permeability.

The furthest possible distance of the weakly coupled proton from Cu^{2+} is 3.8 Å. The intensities of the AB and AB′ resonances in pMMO or DβM do not decrease upon addition of azide or CN (results not shown). Other weakly coupled protons near ν_H are not very well resolved; they are only visible as shoulders in the broad matrix peak. At higher frequency (16.8 MHz) a small broad resonance (C′ in Figures 2A and 2B) is seen, whose low-frequency partner (C) is hardly visible, yielding a hyperfine coupling of 6 MHz, equivalent to a maximum distance of 3.0 Å (eqn 3). It has been reported previously that the intensities at high frequencies can be more pronounced than those at low frequencies [24–26].

In Figures 2(B) and 3(B), it is shown that exchange from H_2O to ^2H_2O results in a decrease in intensities of AB and AB′, indicating that these weakly coupled protons are exchangeable. This suggests that the EPR visible Cu^{2+} site in pMMO is accessible to solvent. As expected at the Larmor frequency ν_D, a novel weak resonance is observed originating from the exchanged deuterons close to the Cu^{2+} site. However, there remain resonances in pMMO (Figure 2B; BB′), especially sharp ones at high frequency. This indicates that weakly coupled protons with coincidentally the same $A(^1H)$ of 2.9 MHz are present, which are not exchangeable by ^2H_2O. In DβM (Figure 3B), the BB′ resonances are split into two lines. For the CC′ resonances, it is not clear if they are partially decreased due to ^2H_2O exchange. The broad line C′ in the vicinity of 16.8 MHz seen in pMMO seems to split into a doublet (Figure 2B). These two latter, much more strongly coupled, protons are apparently not exchangeable.

^{14}N-ENDOR measurements

For the I = 1 nucleus of ^{14}N, one would expect either two or four ENDOR lines. Assuming that the quadrupole splitting P is not resolved, there are two lines centred around either the 'free'-nitrogen NMR frequency (1 MHz at X-band) or half of the ^{14}N-hyperfine interaction value A. Remote, non-co-ordinating nitrogens of histidines are weakly coupled, and thus display

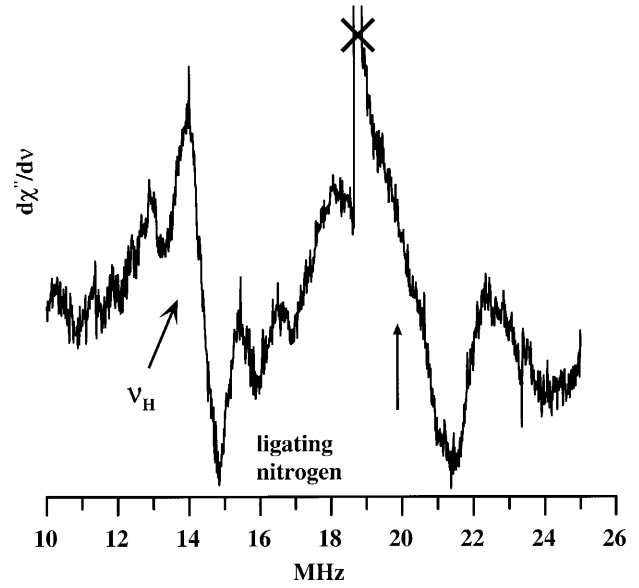

Figure 4 CW ENDOR of DβM in the region 10–26 MHz, showing the resonances of the strongly coupled nitrogens ligating the Cu in the vicinity of 19.8 MHz

The spike (marked with 'X') is an artefact of the instrument. The ENDOR spectrum is measured at the high-field edge of the EPR envelope, as indicated in Figure 1(B), arrow on the right.

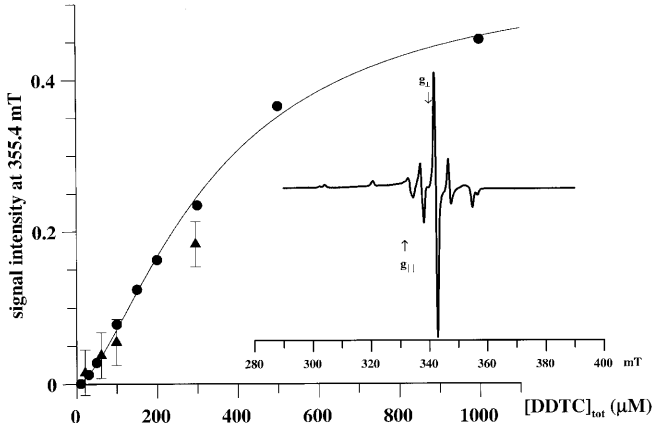

Figure 5 pMMO fragments (80–85 μM Cu^{2+} measured by EPR) were titrated with DDTC

The $Cu(DDTC)_2$ complex formed is soluble in a hydrophobic environment, i.e. the membrane fragments. The spectrum of the $Cu(DDTC)_2$ complex is shown in the inset; the hyperfine structure is indicative of a co-ordination with four sulphurs. The DDTC 'pulls' the EPR visible copper out of pMMO. EPR measurements were done at a temperature of 10K, modulation frequency of 100 kHz and modulation amplitude of 1.0 mT.

resonances centred at the ^{14}N Larmor frequency $\nu_N = 1.04$ MHz, according to $\nu_N \pm A/2$. The remote nitrogens in pMMO, as well as in DβM, can be detected at 0.7 and 1.4 MHz, as shown in Figures 2(A) and 3(A), yielding $A(N^{remote}) = 0.7$ MHz. We compared our results in the low-frequency region with ENDOR spectra of $Cu(imidazole)_4$ and $Cu(NH_3)_4$, for which our instrumental set-up could clearly detect the remote nitrogens of the imidazole complex, whereas the ammonia complex did not show resonances in this region ([26,27], and results not shown). Nitrogens directly co-ordinated to Cu^{2+} show strong hyperfine interaction, and therefore, according to $A/2 \pm \nu_N$, broad resonances are expected, typically $A(^{14}N) \approx 40$ MHz. In Figure 4, the resonances of the strongly coupled nitrogens in DβM are displayed, giving an $A/2$ of 20 MHz, i.e. $A(^{14}N) = 40$ MHz. For pMMO, it was not possible to detect this resonance unambiguously, since the copper concentration is too low and at the high-field edge both the pyrroquinoline quinone radical of the methanol dehydrogenase and the Mn(II) signals interfere. Our CW ENDOR results are in agreement with those obtained by pulsed techniques of pMMO (Bath) and DβM [9,20]. The ENDOR results are also summarized in Table 2.

DDTC titration of pMMO

DDTC is a well-known copper chelator. The complex $Cu(DDTC)_2$ is almost insoluble in water, but it is soluble in hydrophobic solvents, such as chloroform/hexane. Copper is co-ordinated by the four sulphurs of two DDTC ligands, yielding an axial EPR spectrum with A and g values as listed in Table 1 [28]. Chelation of the copper (Figure 5) in pMMO-containing membrane fragments yields an EPR spectrum (inset to Figure 5) that has the same parameters as those of the sole hydrophobic complex in $CHCl_3$/toluene (60:40, v/v; [28]). This indicates that the copper ion is 'pulled out' of its ligating protein environment. Further evidence comes from ENDOR experiments, since the resonances of the remote nitrogens of the previously observed histidine ligands have disappeared (results not shown).

DISCUSSION

The copper site of pMMO is assumed to be the active site of the enzyme complex. The number of coppers involved is a matter of controversy [5–10]. Chan and co-workers [4,10] suggest the existence of trinuclear copper centres with at least 15 Cu per pMMO, whereas Zahn and DiSpirito [5] propose a mononuclear copper site and 12 Cu per pMMO. In the EPR study of Yuan et al. [7], two slightly different type-2 coppers are discussed, one of them co-ordinated by four histidines.

EPR investigation

Here, we investigated membrane fragments containing a large amount of pMMO from *M. capsulatus* (strain M), which expresses only the membrane-bound form of the enzyme [22], with EPR and CW ENDOR spectroscopy. Our membrane preparations with a relatively high specific activity and low copper content might reflect pMMO with less adventitiously bound Cu than that reported earlier, due to the different growth of bacteria at a pH (of 5.6) lower than that used for other methylotrophic bacteria, e.g. *M. capsulatus* (Bath). With the majority of the protein in our membranes arising from pMMO and a low amount of EPR-active Cu^{2+}, it is highly unlikely that our preparations of pMMO contain 15–21 coppers per molecule of pMMO, which has been proposed for pMMO preparations from other species [5–10] with $>$ 6-fold lower specific activity [6,8]. However, membrane fragments with pMMO of *M. capsulatus* (strain M) seem to contain additionally EPR-silent copper, which is strongly bound as the EPR visible copper site. It might be Cu^+ or Cu^{2+} coupled to another, as-yet-unknown, paramagnetic centre. The EPR spectrum of the EPR-active Cu^{2+} site in our preparation is not significantly different from EPR spectra of pMMOs from other species, such as *M. capsulatus* (Bath) or *Methylomicrobium album* BG8 (Table 1, and references therein). Simulations of the resolved superhyperfine lines (Figure

1C) originating from the nitrogenous ligands are in good agreement with three or four histidines co-ordinating the EPR visible type-2 copper, as reported for other pMMOs [7]. The saturated EPR spectrum indicates a minor type-2 copper contamination that is not visible under non-saturating conditions (Figures 1A and 1C). Adventitiously bound copper, i.e. copper bound to lipids, can exhibit a typical type-2 copper spectrum that has no resolved superhyperfine couplings. Thus, from our data, we cannot clearly determine whether there are two slightly different type-2 coppers, as were measured in ref. [7] with S-band EPR spectroscopy. The simulation of the intensities of N-superhyperfines is not influenced by the superimposition of two type-2 copper spectra, where one of them shows no resolved superhyperfines in the perpendicular region.

Oxidation of pMMO

Chan and colleagues [10] reported an increase in the amount of EPR visible Cu^{2+} in pMMO after oxidation with $K_3[Fe(CN)_6]$. The EPR spectrum thus obtained became isotropic, and they suggested the presence of an exchange-coupled trinuclear Cu(II) cluster. For other Cu-containing proteins and pMMOs, formation of novel EPR-active $K_2CuFe(CN)_6$ complexes has been reported [29]. However, incubation of our pMMO with $K_3[Fe(CN)_6]$ did not increase the Cu^{2+} concentration by a factor of two or three, as would have been expected if trinuclear clusters with EPR-silent Cu(I) were present [10,11]. There was no change in either the EPR signal height of Cu(II) or the EPR signal shape. We could not detect any EPR signal from $K_2CuFe(CN)_6$ complexes [29], since our cells and membrane fragments were washed with copper-free buffer and we did not use additional Cu^{2+} during the preparation. The $K_3Fe(CN)_6/K_2Fe(CN)_6$ redox couple has, under similar conditions, a potential of $+410 \pm 20$ mV, which has been used with DβM to determine the redox potential of DβM without problems of formation of $K_2CuFe(CN)_6$ [30]. Thus we cannot on the basis of the results of this ferricyanide oxidation experiment exclude the presence of a copper centre in pMMO with a high redox potential, which occurs in some copper proteins [31]. Furthermore, the microwave power saturation results for our pMMO preparation suggest also that the EPR-active Cu^{2+} is not part in any cluster. Thus our result is best explained in the following manner: the resting EPR-active Cu^{2+} in pMMO is mononuclear and fully oxidized as isolated, and the suggested trinuclear Cu(II) cluster is not present.

Comparison of the behaviour of pMMO and DβM towards inhibitors and chelator DDTC

The EPR spectrum of DβM shows significant differences upon addition of the inhibitors azide and cyanide [19], whereas the EPR spectrum of the copper site of pMMO is unaffected by these small molecules. Here, we suggest that they do not bind to the EPR visible copper site of pMMO. We know that the copper centres of our pMMO (as well as DβM) can be easily chelated by several chelators, as we have shown here for the hydrophilic molecule DDTC, corroborating the accessibility of the EPR visible copper site in pMMO. It is likely that this EPR visible Cu^{2+} site is rather hydrophilic. For a hydrocarbon-binding enzyme, we would expect a hydrophobic site, as, for example, found in sMMO [2]. The dinuclear iron site in sMMO is situated in a hydrophobic pocket, since methane is hydrophobic. There is also the possibility that the actual site of location of the mononuclear Cu^{2+} site in pMMO might be comparable with the location of the Cu_A site of cytochrome *c* oxidase, where it has been shown by ENDOR experimentation that the dinuclear Cu_A site is 5.4 Å (corresponding to $A^H = 2$ MHz) away from the protein–water interface [32]. This distance was corroborated by the crystal structures of cytochrome *c* oxidase [33,34]. Takeguchi et al. [6] proposed the existence of one copper close to the surface of the pMMO, and a second copper buried in the protein, which might be the active-site copper. Taken together, the EPR-active copper in pMMO from *M. capsulatus* (strain M) is both accessible to solvent and strongly bound to the protein. It appears that it is not the site of oxygen binding, but rather is a structural copper or one with an electron-transfer function, which may be situated at the surface of the protein.

Comparison of the CW ENDOR data of pMMO and DβM

X-band CW ENDOR spectra of pMMO were recorded in comparison with ENDOR spectra of the Cu^{2+} site of DβM. For pMMO, which is situated in membrane fragments, the maximal EPR visible Cu^{2+} concentration was only 200 μM. In spite of the different EPR parameters of pMMO and DβM, their ENDOR spectra are almost identical. Compared with ENDOR spectra of the type-2-copper-containing enzyme, superoxide dismutase (SOD), which has histidines as ligands [27,35], similar ^1H interactions ($A = 1$–3 MHz) at field-position $g_\perp$ were found for pMMO. For DβM, these ^1H interactions are not as well resolved. One major ^2H_2O-exchangeable ^1H interaction is seen with $A^H = 2.9$ MHz, indicating the presence of protons in the vicinity of the copper sites in pMMO and DβM. As field-swept ENDOR was not possible due to weak signal intensity, especially in the $g_\parallel$ field region, the superhyperfine tensor could not be determined completely.

The ^1H resonances can be tentatively assigned according to the assignments for SOD and Cu(imidiazole)$_4$ models [26,27]. There are non-exchangeable protons with $A = 6$ MHz, corresponding to a distance of approx. 3.0 Å (eqn 3), which is in good agreement with the $C_\alpha H$ proton of the histidine rings [26]. The exchangeable protons with $A^H = 2.9$ MHz might be the $N_\delta H$ protons of histidine rings and/or alternatively, from an apical water ligand. The NH protons are at a distance of approx. 5 Å [26] from the Cu^{2+}, which does not fit to our calculated distance of 3.8 Å. For a water molecule in an apical position, our calculated Cu-to-H distance of 3.8 Å yields a Cu-to-O distance of about 3.3 Å, which seems reasonable for a loosely bound water. Yuan et al. [7] showed convincingly that one EPR visible copper in pMMO is ligated by four histidines, which, in turn, leaves an apical site for a loosely co-ordinated water. The EPR visible Cu^{2+} site of pMMO may be situated at the protein–water surface, but here, 3.8 Å seems to be relatively short a distance to serve as a criterion for location at the membrane–water interface. It suggests rather the same situation as found in DβM, where the Cu^{2+} site is situated in a water-filled cleft (see below). There are resonances remaining after ^2H_2O exchange ($A^H = 2.9$ MHz) that cannot be assigned to histidines, but which may be protons from the backbone coming close to the Cu^{2+} site.

The identical effect of ^2H_2O exchange on the ENDOR spectra strongly suggests that the EPR visible copper site in pMMO is exposed to water in a similar manner as the Cu^{2+} sites in DβM, on the basis of the known structure of PAMcc [13].

Each of the copper centres in DβM has at least one open co-ordination site that can be occupied by water. Our ENDOR data do not reveal the presence of a strong water ligand very close to the copper site of pMMO and DβM at the field positions measured, since a proton superhyperfine coupling of about 10 MHz could not be detected, as expected for a H_2O ligand strongly co-ordinated to copper shown previously by Atherton

and Horsewill for the $Cu(H_2O)_6^{2+}$ complex [36]. The causes of a lack of a ^{1}H-ENDOR response of protons from a (possible) H_2O ligand might be structural. If the Cu^{2+} is located in a wide cleft, as assumed for DβM, the possible H_2O ligands might be frozen in all possible rotation orientations with respect to the Cu^{2+}, so that the ENDOR response is 'blurred'. The nuclear relaxation of protons of the H_2O ligands might also be unfavourable for the ENDOR measurements. In pMMO, it is possible that only the apical position can be occupied, assuming that the copper is ligated by four histidines, as described previously [7].

Addition of azide or cyanide as small copper ligands does not affect the main ENDOR AB and AB' resonances in DβM or pMMO. N_3^- and CN^- are thought to cause dissociation of a water molecule upon binding to copper. The exchange of one of them by azide or by cyanide might not lead to a significant change in the ENDOR spectrum if the H_2O molecule is only loosely co-ordinated.

Conclusions

We have studied, with EPR and ENDOR spectroscopies, the EPR-active type-2 Cu sites of pMMO and DβM. Our low copper content and relatively high specific activity exclude the presence of 15 or more Cu per pMMO, in agreement with a lack of an effect of addition of the oxidizer $K_3[Fe(CN)_6]$. With ^{1}H-ENDOR spectroscopy, we show the presence of very similar ^2H_2O-exchangeable protons close to the Cu^{2+}; these protons might be located at the water–protein interface for both enzymes. We show a nearly similar strength of the ^{14}N coupling to Cu^{2+} in both enzymes. The EPR-active Cu^{2+} in pMMO is not close to another paramagnetic centre, and cannot be perturbed by known small inhibitors, which together indicates that this copper site has an electron-transfer or structural role, and excludes this copper as part of a trinuclear cluster.

Molecular modelling can be an useful tool for unknown metal-binding sites. On the basis of the primary structure of five different pMMO β-peptides (the 27 kDa subunit) and 12 sequences from the related ammonia mono-oxygenase and model building of transmembrane helices, Tukhvatullin et al. [37] recently published several structural models of the oxygen-activating copper site of pMMO. Tukhvatullin and colleagues showed that, in pMMO, no trinuclear copper clusters could be possible. Of particular interest is the presence of two conserved tyrosines in the pMMO β-peptide [residues 26 and 146 in *M. capsulatus* (Bath)]. It was suggested that they may be ligands of the copper of the pMMO β-peptide in the active site, or close to the metal-binding site [37], but this copper should be the EPR-silent Cu that is observed after hydrogen peroxide or base treatment of our membranes. A speculative hypothesis would be that one of these tyrosines might be oxidized to a tyrosyl radical as a part of the pMMO catalytic cycle, after the transfer of an electron from the EPR-active copper site to the oxygen-activating site. For other copper-containing proteins, such as galactose oxidase, as well as in Photosystem II, the involvement of tyrosines/tyrosyl radicals (or derivatives of tyrosines) in the catalytic mechanism is known [38,39], and has been suggested for cytochrome *c* oxidase [40,41]. In our future studies, the origin of the EPR-silent copper and the involvement of tyrosines in the catalytic cycle will be elucidated.

This work was financed by the Norwegian Research Council (K.K.A.), the TMR programme of EU contract no. ERBMRFXCT980207 for the network called "The iron-oxygen protein network" (K.K.A.). We thank Professor Einar Sagstuen (University of Oslo) for valuable discussions on practical aspects of the ENDOR measurements. B.K. would like to thank Dr Peter P. Schmidt (of our laboratory, present address: Max Planck Institute of Radiation Chemistry, Mülheim a. d. Ruhr, Germany) for helpful discussions.

REFERENCES

1 Klinman, J. P. (1996) Mechanisms whereby mononuclear copper proteins functionalize organic substrates. Chem. Rev. **96**, 2541–2561
2 Wallar, B. J. and Lipscomb, J. D. (1996) Dioxygen activation by enzymes containing binuclear non-heme iron clusters. Chem. Rev. **96**, 2562–2583
3 Dalton, H. (1985) The effect of copper ions on membrane content and methane monooxygenase activity in methanol-grown cells of *Methylococcus capsulatus* (Bath). J. Gen. Microbiol. **131**, 155–163
4 Nguyen, H.-H. T., Shiemke, A. K., Jacobs, S. J., Hales, B. J., Lidstrom, M. E. and Chan, S. I. (1994) The nature of the copper ions in the membranes containing the particulate methane monooxygenase from *Methylococcus capsulatus* (Bath). J. Biol. Chem. **269**, 14995–15005
5 Zahn, J. A. and DiSpirito, A. A. (1996) Membrane-associated methane monooxygenase from *Methylococcus capsulatus* (Bath). J. Bacteriol. **178**, 1018–1029
6 Takeguchi, M., Miyakawa, K. and Okura, I. (1999) The role of copper in particulate methane monooxygenase from *Methylosinus trichosporium* OB3b. J. Mol. Cat. **137**, 161–168
7 Yuan, H., Collins, M. L. P. and Antholine, W. E. (1999) Type 2 Cu^{2+} in pMMO from *Methylomicrobium album* BG8. Biophys. J. **76**, 2223–2229
8 Yuan, H., Collins, M. L. P. and Antholine, W. E. (1997) Low-frequency EPR of the copper in particulate methane monooxygenase from *Methylomicrobium albus* BG8. J. Am. Chem. Soc. **119**, 5073–5074
9 Elliott, S. J., Randall, D. W., Britt, R. D. and Chan, S. I. (1998) Pulsed EPR studies of particulate methane monooxygenase from *Methylococcus capsulatus* (Bath): evidence for histidine ligation. J. Am. Chem. Soc. **120**, 3247–3248
10 Nguyen, H.-H. T., Elliott, S. J., Yip, J. H.-K. and Chan, S. I. (1998) The particulate methane monooxygenase from *Methylococcus capsulatus* (Bath) is a novel copper-containing three-subunit enzyme: isolation and characterization. J. Biol. Chem. **273**, 7957–7966
11 Nguyen, H. T., Nakgawa, K. H., Hedman, B., Elliott, S. J., Lidstrom, M. E., Hodgson, K. O. and Chan, S. I. (1996) X-ray absorption and EPR studies on the copper ions associated with the particulate methane monooxygenase from *Methylococcus capsulatus* (Bath). Cu(I) ions and their implications. J. Am. Chem. Soc. **118**, 12766–12776
12 Abudu, N., Banjaw, M. Y. and Ljones, T. (1998) Kinetic studies on the activation of dopamine β-monooxygenase by copper and vanadium ions. J. Eur. Biochem. **257**, 622–629
13 Southan, C. and Kruse, L. I. (1989) Sequence similarity between dopamine β-hydroxylase and peptide α-amidating enzyme: evidence for a conserved catalytic domain. FEBS Lett. **255**, 116–120
14 Prigge, S. T., Kolhekar, A. S., Eipper, B. A., Mains, R. E. and Amzel, L. M. (1997) Amidation of bioactive peptides: the structure of peptidylglycine α-hydroxylating monooxygenase. Science **278**, 1300–1305
15 Eipper, B. A., Quon, A. S. W., Mains, R. E., Boswell, J. S. and Blackburn, N. J. (1995) The catalytic core of peptidylglycine α-hydroxylating monooxygenase: investigation by site-directed mutagenesis, Cu X-ray-absorption spectroscopy, and electron-paramagnetic-resonance. Biochemistry **34**, 2857–2865
16 Kolhekar, A. S., Keutmann, H. T., Mains, R. E., Quon, A. S. W. and Eipper, B. A. (1997) Peptidylglycine α-hydroxylating monooxygenase: active site residues, disulfide linkages, and a two-domain model of the catalytic core. Biochemistry **36**, 10901–10909
17 Boswell, J. S., Reedy, B. J., Kulathila, R., Merkler, D. and Blackburn, N. J. (1996) Structural investigations on the coordination environment of the active-site copper centers of recombinant bifunctional peptidylglycine α-amidating enzyme. Biochemistry **35**, 12241–12250
18 Blackburn, N. J., Concannon, M., Shahiyan, S. K., Mabbs, F. E. and Collison, D. (1988) Active-site of dopamine β-hydroxylase: comparison of enzyme derivatives containing 4 and 8 copper atoms per tetramer using potentiometry and electron-paramagnetic-resonance-spectroscopy. Biochemistry **27**, 6001–6008
19 Blackburn, N. J., Collison, D., Sutton, J. and Mabbs, F. E. (1984) Kinetic and electron-paramagnetic-resonance studies of cyanide and azide binding to the copper sites of dopamine (3,4-dihydroxyphenethylamine) β-monooxygenase. Biochem. J. **220**, 447–454
20 McCracken, J., Desai, P. R., Papadopoulos, N. J., Villafranca, J. J. and Peisach, J. (1988) Electron spin-echo studies of the copper(II) binding-sites in dopamine β-hydroxylase. Biochemistry **27**, 4133–4137

21 Blackburn, N. J., Hasnain, S. S., Pettingill, T. M. and Strange, R. W. (1991) Copper K-extended X-ray absorption fine-structure studies of oxidized and reduced dopamine β-hydroxylase: confirmation of a sulfur ligand to copper(I) in the reduced enzyme. J. Biol. Chem. **266**, 23120–23127
22 Tukhvatullin, I. A., Korshunova, L. A., Gvozdev, R. I. and Dalton, H. (1996) Investigation of the copper centre of membrane-bound methane monooxygenase from subcellular structures of *Methylococcus capsulatus* (Strain M). Biochemistry (Moscow) **61**, 886–891
23 Smith, D. D. S. and Dalton, H. (1989) Solubilization of methane monooxygenase from *Methylococcus capsulatus* (Bath). Eur. J. Biochem. **182**, 667–671
24 DeRose, V. and Hoffman, B. M. (1995) Electron nuclear double resonance. Methods Enzymol. **246**, 554–589
25 Feher, G. (1970) Electron paramagnetic resonance with applications to selected problems in biology. In Les Houches Lectures, Gordon and Breach, Science Publishers, New York
26 Scholl, H.-J. and Hüttermann, J. (1992) ESR and ENDOR of Cu(II) complexes with nitrogen donors: probing parameters for prosthetic group modeling of superoxide dismutase. J. Phys. Chem. **96**, 9684–9691
27 Reinhard, H., Kappl, R., Hüttermann, J. and Viezzoli, M.-S. J. (1994) ENDOR of superoxide dismutase: structure determination of the copper site from randomly oriented specimen. J. Phys. Chem. **98**, 8806–8812
28 Pilbrow, J. R. (1990) Transition Ion Electron Paramagnetic Resonance, Clarendon Press/Oxford University Press, Oxford
29 Yuan, H., Collins, M. L. P. and Antholine, W. E. (1998) Concentration of Cu, EPR-detectable Cu, and formation of cupric-ferrocyanide in membranes with pMMO. J. Inorg. Biochem. **72**, 179–185
30 Ljones, T., Flatmark, T., Skotland, T., Petersson, L., Bäckström, D. and Ehrenberg, A. (1978) Dopamine β-hydroxylase: electron-paramagnetic resonance and oxidation-reduction properties of enzyme-bound copper. FEBS Lett. **92**, 81–84
31 Solomon, E. I., Sundaram, U. M. and Machonkin, T. E. (1996) Multicopper oxidases and oxygenases. Chem. Rev. **96**, 2563–2605
32 Hansen, P. A., Britt, R. D., Klein, M. P., Bender, C. J. and Babcock, G. T. (1993) ENDOR and ESEEM studies of cytochrome-c-oxidase: evidence for exchangeable protons at the Cu(A) site. Biochemistry **32**, 13718–13724
33 Iwata, S., Ostermeier, C., Ludwig, B. and Michel, H. (1995) Structure at 2.8 Angstrom resolution of cytochrome-c-oxidase from *Paracoccus denitrificans*. Nature (London) **376**, 660–669
34 Tsukihara, T., Aoyama, H., Yamashita, E., Tomizaki, T., Yamaguchi, H., Shinzawa-Itoh, K., Nakashima, R., Yaono, R. and Yoshikawa, S. (1995) Structures of metal sites of oxidized bovine heart cytochrome-c-oxidase at 2.8 Angstrom. Science (Washington, D.C.) **269**, 1069–1074
35 Hüttermann, J., Kappl, R., Banci, L. and Bertini, I. (1988) An ENDOR study of human and bovine erythrocyte superoxide dismutase: H-1 and N-14 interactions. Biochim. Biophys. Acta **956**, 173–188
36 Atherton, N. M. and Horsewill, A. J. (1979) Proton ENDOR of $Cu(H_2O)_6^{2+}$ in $Mg(NH_4)_2(SO_2)_4.6H_2O$. Mol. Phys. **37**, 1349–1361
37 Tukhvatullin, I. A., Gvozdev, R. I. and Andersson, K. K. (2000) The structure of the active center of β-peptide in membrane-bound methane monooxygenase (pMMO) from *Methylococcus capsulatus* Bath. Dokl. Akad. Nauk **374**, 177–182
38 Gerfen, G. J., Bellew, B. F., Griffin, R. G., Singel, D. J., Ekberg, C. A. and Whittaker, J. W. (1996) High-frequency electron paramagnetic resonance spectroscopy of the apogalactose oxidase radical. J. Phys. Chem. **100**, 16739–16748
39 Hoganson, C. W. and Babcock, G. T. (1997) A metalloradical mechanism for the generation of oxygen from water in photosynthesis. Science (Washington, D.C.) **277**, 1953–1956
40 Proshlyakov, D. A., Pressler, M. A., DeMaso, C., Leykam, J. F., DeWitt, D. L. and Babcock, G. T. (2000) Oxygen activation and reduction in respiration: involvement of redox-active tyrosine 244. Science (Washington, D.C.) **290**, 1588–1591
41 MacMillan, F., Kannt, A., Behr, J., Prisner, T. and Michel, H. (1999) Direct evidence for a tyrosine radical in the reaction of cytochrome c oxidase with hydrogen peroxide. Biochemistry **38**, 9179–9184

Received 1 August 2001/14 December 2001; accepted 14 February 2002